Advances in Nano Research, *Vol. 17, No.4 (2024) 293-299*
https://doi.org/10.12989/anr.2024.17.4.293

Microorganisms profile variation in MHD Casson nanofluid: Chemical reaction and Arrhenius energy activation

Muzamal Hussain[1], Mohamed Amine Khadimallah*[2], Humaira Sharif[3] and Elimam Ali[2]

[1]*Department of Mathematics, University of Sahiwal, Sahiwal, 57000, Pakistan*
[2]*Department of Civil Engineering, College of Engineering, Prince Sattam Bin Abdulaziz University, Al-Kharj, 16273, Saudi Arabia*
[3]*Department of Mathematics, Government College University, Faisalabad, 38000, Pakistan*

(*Received April 17, 2024, Revised August 14, 2024, Accepted August 17, 2024*)

Abstract. In this paper, the simplified ordinary differential equations are solved with shooting technique. The concentration and microorganism slip boundary conditions are implemented. Non-linear expression is reduced via non-dimensional variables. The microorganism distribution declines by increasing Lewis number and microorganism slip parameter. Behavior of distinct influential parameters viz: Eckert number, bioconvected Lewis number, bioconvected Peclet number, microorganisms slip parameter are investigated graphically and analyzed for concentration and microorganism. Enhanced concentration is correlated with energy activation. An acceptable agreement is reached when the numerical technique is compared to the existing literature. The magnitude of microorganism transfer rate shows decreasing behavior for higher values of slip parameters.
Keywords: bioconvected Lewis number; bioconvected Peclet number; Eckert number; microorganisms slip parameter

1. Introduction

Recently, convection via gyrotactic microorganisms is flourishing huge response on account of their utilization in microfluidic appliances such as bio-sciences dispersion, bio-galvanic devices, in microbial oil recovery and formulation of gas and oil transfer sedimentary bowls. Nanofluids can vary the thermal characteristics as well as transport of the carrier liquid and consequently increase mass as well as thermal and motile microorganism transportation. These liquids are colloids containing base fluid like water and nanosize particles like non-metallic and metallic particles. Firstly, Wang 1988 studied the fluid behavior along the stretching cylinder. The detailed study of fluid flow along the stretched cylinder for the boundary layer was made (Ishak and Nazar 2009) regarding. Wang 2011 obtained asymptotic solutions for high Reynold number using slip flow condition. (Salahuddin *et al*. 2017). The effects of Soret and Dufour for the Casson fluid by considering the heat Mixed convection condition together with slip flow and obtained numerical solution for the boundary layer problem of Williamson fluid flow over a stretching cylinder transfer along stretching cylinder was worked out (Mahdy 2015). A revolutionary high performance multi-walled carbon nano-polyvinylpyrrolidone/ silicon-based shear thickening fluid (MWCNTs-PVP/SiO2-STF), later shortened to MPS-STF, was created by Sun *et al*. in 2024. According to Zhu *et al*. (2024), partial differential equations (PDEs) are commonly used to describe nonlinear processes that are seen in a variety of scientific disciplines, such as fluid dynamics, plasma physics, and biology. The uniform suction/blowing effects together with transfer of heat outside the permeable stretching cylinder were considered (Ishaq *et al*. 2008). Recently, there has been an increasing amount of interest in exploring the field of nonlinear partial differential equations in pursuit of solitary wave solutions. This project represents an interesting and difficult field of study (Zhu *et al*. 2024). Practically it is almost impossible to have such fluid which is free from any kind of impurity. Every naturally occurring fluid contains dust particles. Many engineering and industrial problems deal with dusty fluid such as powder mechanization and centrifugal technique to the detachment of particles from the fluid. Flow of dusty fluid can be viewed in many natural phenomena e.g. flow of mud in rivers, blood flow and atmospheric flow during haze. Initiative study of motion of dust particles in laminar flow has been carried out (Saffman, 1962). In wind tunnel studies, the effect of oscillatory fluids on the flow caused by after body vortices which resemble high-speed train vortices was examined (Chen *et al*. 2024).

A viscous, incompressible continuous flow of dusty fluid under the influence of a pressure gradient between two coaxial spinning cylinders was analyzed. The nonlinear free vibration analysis of thin laminated plates sitting on nonlinear elastic foundations was studied geometrically by Akgoz and Civalek (2011). The foundation model of Winkler-Pasternak type is employed.

Using nonlinear theory of the von Karman type, governing equations of motion are produced. The discretized equations of motion for plates are obtained using the discrete singular convolution method. Batou *et al*. (2019) used the novel Higher Shear Deformation Theory (HSDT), which is based on two-dimensional (2D) elasticity

*Corresponding author, Assistant Professor, Ph.D.,
E-mail: am.khadimallah@gmail.com;
mohamedamine.khadimallah@fsgf.rnu.tn

ISSN: 2287-237X (Print), 2287-2388 (Online)

theory, to study the wave propagations in sigmoid functionally graded (S-FG) plates. Compared to earlier shear deformation theories and other higher shear deformation theories, the current higher order theory contains fewer unknowns just four and does not require a shear corrector.

The dependable and precise approach of computationally aided design procedures of advanced thin walled structures in the automotive industries was examined by Baaskaran *et al*. (2018) in order to maximize the use of smart materials with increased energy absorption under dynamic compression loading. To lessen the effects of variable cross section in crash behavior and energy absorption characteristics, the most adaptable components thin walled crash tubes with various geometrical profiles are introduced. The flow of dusty gas in a boundary layer-occupied area was studied (Chakrabarti 1974). Agranat (1988) researched the heat transfer and coefficient of friction for dusty boundary layer flow with pressure gradient. The vibration of a post-buckled fluid-conveying pipe composed of functionally graded material was examined by Selmi and Hassis in 2021. It is believed that the properties of the pipe material are graded according to a power-law distribution in the thickness direction. With different boundary conditions, a precise solution for the fluid-conveying functionally graded pipe's post-buckling deformation is obtained. Su *et al*. (2024) introduced a creative numerical modeling framework that can generate remarkably accurate and efficient 3D mesoscale multi-phase concrete models with unprecedented realism. Many researchers also looked at dusty fluid flow along cylinders in addition to these studies on heat transfer and flow for dusty fluids along sheets or surfaces. Results from a variety of physical parameters were presented along with a discussion of the viscous, incompressible gas flow containing dust particles for an isothermal cylinder (Rebhi 2010). The energy absorption properties of a lattice-web reinforced composite sandwich cylinder (LRCSC), made of ceramsite filler, GFRP face sheets, GFRP lattice webs, and polyurethane (PU) foam, were investigated by Chen *et al*. (2019a, b). The immersed boundary approach is used to study the vortex-induced vibration of three circular cylinders (all of diameter D) arranged equilaterally in a triangle. Huang *et al*. (2024) investigated the steel-hollow core partially encased composite spliced frame beam (SHSFB) and middle partially encased composite brace (MPECB), which exhibit potential for lowering steel use while displaying greater performance. Using a refined theory based on secant functions, Abdulrazzaq *et al*. (2020) examined the thermo-elastic buckling of small-scale functionally graded material (FGM) nano-size plates with clamped edge conditions resting on an elastic substrate exposed to uniformly, linearly, and non-linearly temperature distributions. The FGM nano-size plate's material characteristics exhibit an exponential gradation throughout the thickness of the plate. In a composite beam composed of CFRP plate, SFRC, and conventional concrete (OC), Zhang *et al*. (2023) examined the characteristics of steel fiber reinforced concrete (SFRC), which has a high tensile strength, and carbon fiber reinforced plastic (CFRP), which is lightweight and strong.

Civalek (2017) studied the free vibration analysis of annular plates and conical and cylindrical shells composed of functionally graded materials (FGMs) and composite laminated materials. For FGM, a composite case reinforced with carbon nanotubes (CNTR) is also being considered. Using the transverse shear deformation theory and Hamilton's principle, the equations of motion for a conical shell are produced. Using multi-step DTM, some insightful findings about the heat transfer of a dusty fluid over a hollow extending cylinder were published (Rasekh *et al*. 2013). Zhang *et al*. (2023) examined the mechanical and microstructural properties of alkali-activated composites incorporating nanoparticles. The effects of viscosity and thermal conductivity on the conduction of dusty fluid flow along a stretching cylinder were handled numerically (Konch and Hazarika 2017). Zhang *et al*. (2023) conducted an analysis in 2024 using both computational and experimental methods to examine the flexural performance of UHPC-RC hybrid beams.

The effects of Reynolds number Re (= 50–200) on the flows around a single cylinder and two tandem (center-to-center separation $L^*= L/D= 4$) cylinders, each with a diameter of D, were studied by Derakhshandeh *et al*. (2020). We present and discuss vorticity structures, Strouhal numbers, and time-mean and fluctuating forces. Salah *et al*. (2019) investigated the thermal buckling characteristics of sandwich plates made of functionally graded material (FGM) using a straightforward four-variable integral plate theory. The effect of transverse shear deformations is one of the integral factors taken into account in the suggested kinematics.

In some fresh attempts, the researchers have pondered over new dimensions of stretching i.e., exponentially stretching cylinder. The detailed study of flow and transfer of heat for hyperbolic tangent fluid over a stretching cylinder exponentially in vertical direction was carried out (Naseer *et al*. 2014). The difficult problem of applying the machine learning model's merit to the multi-objective optimization (MOO) problem was examined by Huang *et al*. in 2022. The surrogate model will inevitably overfit due to the small amount of training data, which could trick the search engine. Lateral load testing was done on seventeen wood wall frames in two sections by Shadravan *et al*. (2019). Eight tests were conducted in Section I using the ASTM E564 test technique to examine the structural foam sheathing of shear walls subjected to monotonic loads.

Similarity solution has been derived for steady boundary layer and heat flow of Casson nanofluid (Malik *et al*. 2013) while cylinder was stretching exponentially along its radius. The flow of Micropolar fluid through vertical exponentially stretching cylinder along the axial direction and discussed heat transfer effects, too, were considered (Rehman *et al*. 2015). The cyclic performance of new composite beam-to-column connections with fewer beam section fuse elements was examined by Yao *et al*. in 2023. Recently, several researchers employed several techniques for nonlinear modeling (Eltaher *et al*. 2019, Ebrahimi *et al*. 2019, Safaei *et al*. 2019, Shahsavari *et al*. 2019, Benmansour *et al*. 2019, Asghar *et al*. 2020, Hussain and Naeem 2019, Fatahi-Vajari *et al*. 2019, Khadimallah *et al*. 2020a, b, Banoqitah *et al*.

2022, Hussain 2022, Qazaq *et al*. 2022, Muzamal 2022, Arshad *et al*. 2024, Hussain *et al*. 2020a, b, 2024).

In this paper, the steady incompressible Darcy-Forchheimer boundary layer flow of MHD bioconvection Casson type nanofluid by nonlinear stretchable surface with different parameters. No such investigation is reported till date. Shooting method is a tool for its numerical achievements. Many physical and mathematical problems yield highly non-linear differential equations and their exact results are not commonly possible. To evaluate such type of equations numerically, one of the powerful method is to obtained the solution of such problems is shooting technique. This technique is simple, elegant and without any difficult discretization approach. One of the exclusive quality of this approach is that missing boundary value conditions can be started by utilizing smart initial guesses. For better accuracy of solution convergence is investigated by utilizing this method. Impact of relevant physical parameters, like Eckert number, bioconvected Lewis number, bioconvected Peclet number, microorganisms slip parameter versus concentration and microorganisms profile are studied and shown through plots.

2. Mathematical formulation

The cluster of nanosize particles is ignored, the nanoparticles suspension is assumed to be stable compound that is essential for the presence of motile microorganisms. The surface having stretchable velocity U_w with x-axis and n denotes the non-linearity in surface stretching rate i.e., $u_w(x) = cx^n$. At free surface zero velocity is observed. To emphasize the thermo-physical characteristics, a uniform magnetic field is considered for the fluid. To decline the impact of induced magnetic effect, a small Reynolds number is involved. The x-axis is directed towards the nonlinear stretching surface and y-axis is taken normal to the x-axis. Attributes of Brownian dissemination and thermophoresis are additionally attended. For an incompressible and isotropic flow the rheological equation of state for Casson type nanofluid is exhibit as

$$\tau_{ij=}\begin{cases} 2\left(\mu_B+\dfrac{P_y}{\sqrt{2\pi}}\right)e_{ij}, & \pi \succ \pi_c \\ 2\left(\mu_B+\dfrac{P_y}{\sqrt{2\pi_c}}\right)e_{ij}, & \pi \prec \pi_c \end{cases} \quad (1)$$

where π denotes the component product of the deformation rate with itself, μ_B is dynamic viscosity of fluid, P_y is the yield fluid stress, π_c is critical value of component product of tensor rate of strain with itself. We assume viscous incompressible Darcy-Forchheimer Casson type nanofluid flow saturating the permeable media by a nonlinear stretching surface. Moreover, the concentration equation is modified by including chemical reaction and Arrhenius energy activation with fitted constant rate m and reaction rate ${K_r}^2$. The governing equations under approximation of boundary layer can be described as (Buongiorno 2006).

$$\frac{\partial u}{\partial x}+\frac{\partial v}{\partial y}=0 \quad (2a)$$

$$u\frac{\partial u}{\partial x}+v\frac{\partial u}{\partial y}=\nu\left(1+\frac{1}{\beta}\right)\frac{\partial^2 u}{\partial y^2}-\left[\frac{\sigma {B_0}^2}{\rho}-\frac{\nu}{K'}\right]u - \frac{\overline{C_b}}{\sqrt{k}}u^2 \quad (2b)$$

$$u\frac{\partial T}{\partial x}+v\frac{\partial T}{\partial y}=\alpha\frac{\partial^2 T}{\partial y^2}+\tau^*\left[\frac{\partial C}{\partial y}\frac{\partial T}{\partial y}D_{Br}+\left(\frac{\partial T}{\partial y}\right)^2\frac{D_{Th}}{T_\infty}\right] + \frac{\mu}{\rho C_p}\left(1+\frac{1}{\beta}\right)\left(\frac{\partial u}{\partial y}\right)^2 \quad (2c)$$

$$u\frac{\partial C}{\partial x}+v\frac{\partial C}{\partial y}= \frac{D_{Th}}{T_\infty}\frac{\partial^2 T}{\partial y^2}+D_{Br}\frac{\partial^2 C}{\partial y^2}-{K_r}^2(C-C_\infty)\left(\frac{T}{T_\infty}\right)^m exp\left(\frac{-E_a}{k_B T}\right) \quad (2d)$$

$$u\frac{\partial N}{\partial x}+v\frac{\partial N}{\partial y}+\frac{bW_c}{(C_w-C_\infty)}\left[\frac{\partial}{\partial y}\left(N\frac{\partial C}{\partial y}\right)\right]=D_n\left(\frac{\partial^2 N}{\partial y^2}\right) \quad (2e)$$

Here, (u, v) are velocities component in (x, y) directions, respectively. The slip boundary conditions are:

$$u=U_w=cx^n+M_1\left(1+\frac{1}{\beta}\right)\frac{\partial u}{\partial y}, T=T_w+M_2\frac{\partial T}{\partial y}, C=C_w+M_3\frac{\partial C}{\partial y}, N=N_w+M_4\frac{\partial N}{\partial y}, v=0, \text{ as } y=0 \quad (3a)$$

$$u\to 0, T\to T_\infty, C\to C_\infty, N\to N_\infty, \text{ as } \quad y\to\infty, \quad (3b)$$

where $M_1(x)=M_0x^{-\left(\frac{n-1}{2}\right)}$, $M_2(x)=N_0x^{-\left(\frac{n-1}{2}\right)}$, $M_3(x)=L_0x^{-\left(\frac{n-1}{2}\right)}$, $M_4(x)=P_0x^{-\left(\frac{n-1}{2}\right)}$ are slip parameters for velocity, temperature, nanoparticles concentration and microorganism's distributions. M_o, N_o, L_o and P_o are constants. μ is dynamic viscosity, ν is kinematic viscosity, σ is electrical conductivity, ρ is base fluid density, $F=\frac{\overline{C_b}}{\sqrt{k}}$ is inertial factor, K' is permeability coefficient of porous media, τdenotes ratio of nanosize particles heat capacity and heat capacity of base fluid, D_{Br} is Brownian diffusion, $\alpha$is temperature diffusivity, D_{Th} is thermophoretic effect, $c\succ 0$ is stretchable rate, N_∞, T_∞, C_∞ are ambient microorganisms, thermal and concentration distributions, B_o is magnetic field effect. We considered the following transformation variables:

$$\eta=\frac{1}{2}\sqrt{\frac{2\rho c(n+1)}{\mu}}x^{\frac{n-1}{2}}y, \quad v=-\frac{1}{2}\sqrt{2c\nu(n+1)}x^{\frac{n-1}{2}}\left[\frac{(n+1)f+(n-1)f'\eta}{n+1}\right], \quad u=cx^nf', \quad \theta(\eta)(T_w-T_\infty)=T-T_\infty, \quad \phi(\eta)(C_w-C_\infty)=C-C_\infty, \quad N(\eta)(N_w-N_\infty)=N-N_\infty \quad (4)$$

By using the above mentioned transformation in Eqs. (2) to (8), we get:

$$f''' + \left(\frac{\beta}{\beta+1}\right) ff'' - Fr\left(\frac{2}{n+1}\right)\left(\frac{\beta}{\beta+1}\right) f'^2 - M\left(\frac{2}{n+1}\right)\left(\frac{\beta}{\beta+1}\right) f' + \lambda\left(\frac{2}{n+1}\right)\left(\frac{\beta}{\beta+1}\right) f' - \left(\frac{2n}{n+1}\right)\left(\frac{\beta}{\beta+1}\right) f'^2 = 0, \quad (5)$$

$$\theta'' + Nb\, Pr\, \theta'\, \phi' + Nt\, Pr\, \theta'^2 + Pr\, f\, \theta' + (1+\frac{1}{\beta}) E_c f''^2 = 0, \quad (6)$$

$$\phi'' + \frac{Nt}{Nb}\theta'' + Le\, Pr\, f\, \phi' - (Le)\, Pr\left(\frac{2}{n+1}\right)\gamma^*(1+\Omega^*\theta)^m\, exp\left(\frac{-E}{1+\Omega^*\theta}\right)\phi = 0, \quad (7)$$

$$N'' + LbfN' - Pe[\phi''(N+\delta_1) + N'\phi'] = 0, \quad (8)$$

$$f(0) = 0, f'(0) = 1 + \alpha\,(1+\frac{1}{\beta}) f''(0), \quad \theta(0) = 1 + \gamma\theta'(0), \phi(0) = 1 + \sigma\phi'(0), \quad N(0) = 1 + \delta N'(0), \text{ at } \eta = 0, \quad (9)$$

$$f'(\infty) \to 0, \theta(\infty) \to 0, \phi(\infty) \to 0, N(\infty) \to 0, \text{ at } \eta \to \infty, \quad (10)$$

Here, α is velocity slip parameter, $\gamma$is temperature slip parameter, σ is nanoparticles concentration slip parameter, δ is microorganisms slip parameter, M is magnetic parameter, Fr is Forchheimer parameter, λ is porosity parameter, Le is Lewis number, Pr denotes the Prandtl number, Nt is thermophoretic parameter, Nb denotes the Brownian factor, Ec is Eckert number, λ^* is chemical reaction factor, E denotes energy activation, Lb is bioconvected Lewis number, Pe is bioconvected Peclet number. Mathematically,

$$\alpha = M_1 x^{\frac{n-1}{2}}\sqrt{\frac{c(1+n)}{2\nu}},\ \gamma = M_2 x^{\frac{n-1}{2}}\sqrt{\frac{c(1+n)}{2\nu}},\ \sigma = M_3 x^{\frac{n-1}{2}}\sqrt{\frac{c(1+n)}{2\nu}},\ \delta = M_4 x^{\frac{n-1}{2}}\sqrt{\frac{c(1+n)}{2\nu}},\ M = \frac{\sigma {B_o}^2}{c\rho x^{n-1}},\ Ec = \frac{{u_w}^2}{c_p(T_w - T_\infty)},\ Fr = \frac{x\overline{C_b}}{\sqrt{k}},\ \lambda = \frac{\nu}{K' c x^{n-1}},\ Le = \frac{\nu}{D_{Br}},\ E = \frac{E_a}{kT_\infty},\ Pr = \frac{\nu}{\alpha},\ Nb = \tau D_{Br}(\nu^{-1}C_w - \nu^{-1}C_\infty),\ Nt = \frac{D_{Th}(\tau T_w - \tau T_\infty)}{\nu T_\infty},\ \gamma^* = \frac{{k_r}^2}{c x^{n-1}},\ Lb = \frac{\nu}{D_m},\ Pe = \frac{bW_c}{D_m},\ \delta_1 = \frac{N_\infty}{N_w - N_\infty} \quad (11)$$

The physical quantities are local motile number, Sherwood number, Nusselt number and skin friction coefficient expressions are defined as:

$$N_n = \frac{-x}{(N_w - N_\infty)}\left(\frac{\partial N}{\partial y}\right)_{y=0},\quad Shr = \frac{-x}{(C_w - C_\infty)}\left(\frac{\partial C}{\partial y}\right)_{y=0},\quad Nu = \frac{-x}{(T_w - T_\infty)}\left(\frac{\partial T}{\partial y}\right)_{y=0}, \quad (12)$$

$$Cf_x = \frac{1}{\rho {u_w}^2}\left(\mu_\beta\left(1+\frac{1}{\beta}\right)\left(\frac{\partial u}{\partial y}\right)_{y=0}\right)$$

In terms of non-dimensional variables reduced density number of microorganisms, reduced Sherwood number, reduced Nusselt number and skin friction coefficient are as follows:

$$Cf_x\, Re_x^{\ \frac{1}{2}} = \left(\frac{n+1}{2}\right)^{\frac{1}{2}}\left(1+\frac{1}{\beta}\right) f''(0),\quad Nu_x\, Re_x^{\ \frac{-1}{2}} = -\left(\frac{n+1}{2}\right)^{\frac{1}{2}}\theta'(0),\quad Sh_x\, Re_x^{\ \frac{-1}{2}} = -\left(\frac{n+1}{2}\right)^{\frac{1}{2}}\phi'(0),\quad Nn_x\, Re_x^{\ \frac{-1}{2}} = -\left(\frac{n+1}{2}\right)^{\frac{1}{2}} N'(0), \quad (13)$$

where $Re_x = \frac{x u_w}{\nu}$ denotes the Reynolds number. The RK (Runge-Kutta) method is widely used for determining the initial- value problems. RK method is very stable, self-starting and very easy to implement.

$$\begin{aligned}
&y_1 = y_1\\
&y_1' = y_2\\
&y_1'' = y_2' = y_3\\
&y_3' = \left(\frac{\beta}{\beta+1}\right)\left[\begin{array}{l} Fr\left(\frac{2}{n+1}\right) {y_2}^2 - y_1 y_3 \\ +M\left(\frac{2}{n+1}\right) y_2 + \lambda\left(\frac{2}{n+1}\right) y_2 + \left(\frac{2n}{n+1}\right) {y_2}^2 \end{array}\right]\\
&y_4 = y_4\\
&y_4' = y_5\\
&y_5' = -\Pr\left[y_1 y_5 + Nb y_5 y_7 + Nt {y_5}^2\right] - \left(1+\frac{1}{\beta}\right) Ec\, {y_3}^2\\
&y_6 = y_6\\
&y_6' = y_7\\
&y_7' = -Le\, Pr\, y_1\, y_7 - \left(\frac{Nt}{Nb} y_5'\right)\\
&\quad +Le\, Pr\left(\frac{2}{n+1}\right)\gamma^*(1+\Omega^* y_4)^m\, exp\left(\frac{-E}{1+\Omega^* y_4}\right) y_6\\
&y_8 = y_8\\
&y_8' = y_9\\
&y_9' = -Lb y_1 y_9 + Pe[(y_8+\delta_1) y_7' + y_7 y_9]
\end{aligned} \quad (14)$$

With the transformed conditions (9) and (10):

$y_1(0) = 0, y_2(0) = 1 + \alpha\left(1+\frac{1}{\beta}\right) y_3(0),\ \ y_4(0) = 1 + \gamma y_5(0), y_6(0) = 1 + \sigma y_7(0),\ y_8(0) = 1 + \delta y_9(0)$ as $\eta \to 0 y_2(\infty) \to 0, y_4(\infty) \to 0, y_6(\infty) \to 0,\ \ y_8(\infty) \to 0,$ as $\eta \to \infty$

For the residual of continuous outcomes erratum control and mesh section provided for all the calculations.

3. Result and discussion

The shooting method is used in this part to solve the non-linear mathematical problem using a numerical scheme. Table 1 displayed to validate the current solutions with

Table 1 Comparison results for Nusselt number with distinct values of $Nb$and Nt for $\beta \to \infty$, n =1, $Fr = \lambda = M = \alpha = \gamma = \sigma = \delta = Pe = Lb = Ec = 0$, $Pr = Le$ =10

Nb	Nt	(Khan and Pop 2010)	Present results
	0.1	0.2522	0.2522
0.20	0.2	0.1816	0.1816
	0.3	0.1355	0.1355
	0.1	0.1194	0.1194
0.30	0.2	0.0859	0.0859
	0.3	0.0641	0.0641

Table 2 Numerical values of motile microorganisms for different values of parameters

α	γ	σ	δ	Nt	Nb	Lb	Pe	$-N'(0)$
0.5								0.8104
0.7	0.5	0.5	0.5	0.1	0.2	0.5	0.5	0.6905
0.9								0.6876
	0.5							0.5344
	0.6							0.5318
	0.7							0.5387
		0.1						0.5742
		0.5						0.5208
		1.0						0.5081
			0.1					0.9501
			0.5					0.8104
			0.7					0.7550
				0.1				0.5417
				0.2				0.5074
				0.3				0.4991
					0.1			0.7535
					0.2			0.7414
					0.3			0.7601
						0.3		0.7091
						0.5		0.7526
						0.7		0.8165
							0.3	0.7244
							0.5	0.7487
							0.7	0.8121

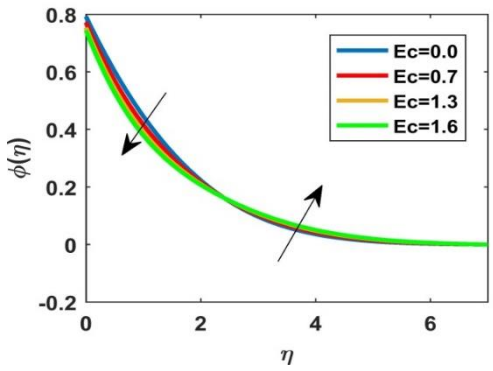

Fig. 1 Concentration profile for variation of $\boldsymbol{Ec}$

previous published literature in specific cases. We noted that present results have excellent agreement with previous results by (Khan and Pop 2010) in specific case. Numerical values of motile microorganisms for distinct parameters are shown in Table 1. From Fig. 1 it is clear that the concentration

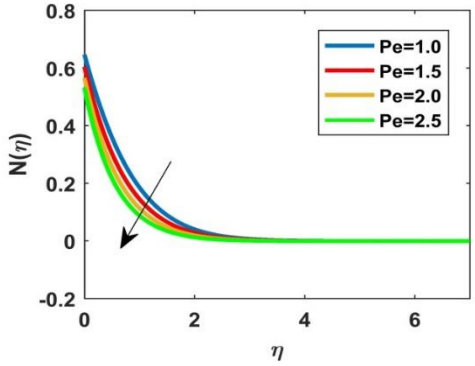

Fig. 3 Microorganisms profile for variation of Pe

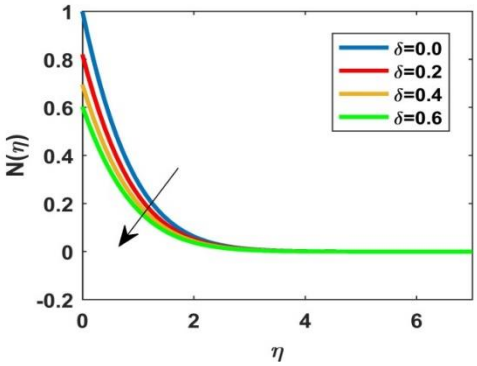

Fig. 4 Microorganisms profile for variation of δ

ϕ decreases for higher values of Ec near the sheet, whereas the opposite trend is examined away from the sheet. Influence of Bioconvection Lewis number Lb on micro-organisms N is displayed in Fig. 2. Reducing behavior of N is inspected as the higher values of Lb. This behavior is occurring due to highest values of Pe the speed of swimming -cell is increased. This maximum speed of swimming –cell is responsible in the weaker behavior of N. Fig. 3 illustrated the impact of Lb on microorganisms N. The retarded behavior of$N$is noted for augmented values of Lb. This happened due to lower microorganism's diffusivity. For maximum values of Lb the weaker diffusivity, due to which microorganisms N is retarded. Fig. 4 execute that the higher values of microorganisms slip parameter δ implies to greater curves of microorganisms N. The micro-organisms profile N is decreasing at wall due to higher values of δ.

4. Conclusions

The steady incompressible Darcy-Forchheimer boundary layer flow of MHD bioconvection Casson type nanofluid by nonlinear stretchable surface with slip conditions has been investigated numerically. The impact of distinct parameters on temperature, velocity, concentration and micro-organism's profiles are examined via tables and graphs. The validity of the current investigation is authorized through comparing the existing outcomes with previous published literature. Reducing behavior of microorganisms profile is inspected

as the higher values of bioconvected Lewis number. The retarded behavior of microorganisms profile is noted for augmented values of bioconvected Lewis number. This happened due to lower microorganism's diffusivity. The microorganisms profile is decreasing at wall due to higher values of microorganisms slip parameter. The bioconvection Lewis number and Peclet number causes to decrease the microorganisms density.

Acknowledgment

This study is supported via funding from Prince Satam bin Abdulaziz University project number (PSAU/2024/R/1446)

References

Abdulrazzaq, M.A., Fenjan, R.M., Ahmed, R.A. and Faleh, N.M. (2020), "Thermal buckling of nonlocal clamped exponentially graded plate according to a secant function based refined theory", *Steel Compos. Struct.*, **35**(1), 147-157. https://doi.org/10.12989/scs.2020.35.1.147

Agranat, V.M. (1988), "Effect of pressure gradient on friction and heat transfer in a dusty boundary layer", *Fluid Dyn.*, **23**, 729-732. http://doi.org/10.1007/BF02614150

Akgoz, B. and Civalek, O. (2011)", Nonlinear vibration analysis of laminated plates resting on nonlinear two-parameters elastic foundations", *Steel Compos. Struct.*, **11**(5), 403-421. https://doi.org/10.12989/scs.2011.11.5.403

Arshad, R., Jalil, M., Hussain, M. and Tounsi, A. (2024), "A novel framework for the construction of cryptographically secure S-boxes", *Comput. Concr.*, **34**(1), 79-91. https://doi.org/10.12989/cac.2024.34.1.079

Asghar, S., Naeem, M.N. and Hussain, M. (2020), "Non-local effect on the vibration analysis of double walled carbon nanotubes based on Donnell shell theory", *Physica E*, **116**, 113726. https://doi.org/10.1016/j.physe.2019.113726

Baaskaran, N., Ponappa, K. and Shankar, S. (2018), "Assessment of dynamic crushing and energy absorption characteristics of thin-walled cylinders due to axial and oblique impact load", *Steel Compos. Struct.*, **28**(2), 179-194. https://doi.org/10.12989/scs.2018.28.2.179

Banoqitah, E.M., Hussain, M., Khadimallah, M.A., Ghandourah, E., Yahya, A., Basha, M. and Alshoaibi, A. (2022), "A simplified directly determination of natural frequencies of CNT: Via aspect ratio", *Adv. Nano Res.*, **13**(3), 207. https://doi.org/10.12989/anr.2022.13.3.207

Batou, B., Nebab, M., Bennai, R., Atmane, H.A., Tounsi, A. and Bouremana, M. (2019), "Wave dispersion properties in imperfect sigmoid plates using various HSDTs", *Steel Compos. Struct.*, **33**(5), 699-716. https://doi.org/10.12989/scs.2019.33.5.699

Benmansour, D.L., Kaci, A., Bousahla, A.A., Heireche, H., Tounsi, A., Alwabli, A.S., Alhebshi, A.M., Al-ghmady, K. and Mahmoud, S.R. (2019), "The nano scale bending and dynamic properties of isolated protein microtubules based on modified strain gradient theory", *Adv. Nano Res.*, **7**(6), 443-457. https://doi.org/10.12989/anr.2019.7.6.443

Chakrabarti, K.M. (1974), "Note on Boundary layer in a dusty gas", *Am. Inst. Aeronaut. Astronaut. J.*, **12**, 1136-1137. http://doi.org/10.2514/3.49427

Chen, J., Zhuang, Y., Fang, H., Liu, W., Zhu, L. and Fan, Z. (2019a), "Energy absorption of foam-filled lattice composite cylinders under lateral compressive loading", *Steel Compos. Struct.*, **31**(2), 133-148. https://doi.org/10.12989/scs.2019.31.2.133

Chen, W., Ji, C., Alam, M. M. and Xu, D. (2019b)", Flow-induced vibrations of three circular cylinders in an equilateral triangular arrangement subjected to cross-flow", *Wind Struct.*, **29**(1), 43-53. https://doi.org/10.12989/was.2019.29.1.043

Chen, X., Zhong, S., Liu, T., Ozer, O. and Gao, G. (2024), "Manipulation of the flow induced by afterbody vortices using sweeping jets", *Phys. Fl.*, **36**(3), 035147. https://doi.org/10.1063/5.0196427

Civalek, Ö. (2017), "Free vibration of carbon nanotubes reinforced (CNTR) and functionally graded shells and plates based on FSDT via discrete singular convolution method", *Compos. Part B Eng.*, **111**, 45-59. https://doi.org/10.1016/j.compositesb.2016.11.030

Derakhshandeh, J.F. and Alam, M.M. (2020), "Reynolds number effect on the flow past two tandem cylinders", *Wind Struct.*, **30**(5), 475-483. https://doi.org/10.12989/was.2020.30.5.475

Ebrahimi, F., Dabbagh, A., Rabczuk, T. and Tornabene, F. (2019), "Analysis of propagation characteristics of elastic waves in heterogeneous nanobeams employing a new two-step porosity-dependent homogenization scheme", *Adv. Nano Res.*, **7**(2), 135. https://doi.org/10.12989/anr.2019.7.2.135

Eltaher, M.A., Almalki, T.A., Ahmed, K.I. and Almitani, K.H. (2019), "Characterization and behaviors of single walled carbon nanotube by equivalent-continuum mechanics approach", *Adv. Nano Res.*, **7**(1), 39. https://doi.org/10.12989/anr.2019.7.1.039

Fatahi-Vajari, A., Azimzadeh, Z. and Hussain, M. (2019), "Nonlinear coupled axial–torsional vibration of single-walled carbon nanotubes using homotopy perturbation method", *Micro Nano Lett.*, **14**(14), 1366-1371. https://doi.org/10.1049/mnl.2019.0203

Huang, H., Xue, C., Zhang, W. and Guo, M. (2022), "Torsion design of CFRP-CFST columns using a data-driven optimization approach", *Eng. Struct.*, **251**, 113479. https://doi.org/10.1016/j.engstruct.2021.113479

Hussain, M. (2022), "Controlling of ring based structure of rotating FG shell: Frequency distribution", *Adv. Concr. Constr.*, **14**(1), 35-43. https://doi.org/10.12989/acc.2022.14.1.035

Hussain, M. (2024), *Small-scale Computational Vibration of Carbon Nanotubes: Composite Structure*, CRC Press.

Hussain, M. and Naeem, M.N. (2019), "Effects of ring supports on vibration of armchair and zigzag FGM rotating carbon nanotubes using Galerkin's method", *Compos. Part B Eng.*, **163**, 548-561. https://doi.org/10.1016/j.compositesb.2018.12.144

Hussain, M., Naeem, M.N., Asghar, S. and Tounsi, A. (2020a), "Theoretical impact of Kelvin's theory for vibration of double walled carbon nanotubes", *Adv. Nano Res.*, **8**(4), 307-322. https://doi.org/10.12989/anr.2020.8.4.307

Hussain, M., Naeem, M.N., Khan, M.S. and Tounsi, A. (2020b), "Computer-aided approach for modelling of FG cylindrical shell sandwich with ring supports", *Comput. Concr.*, **25**(5), 411-425. https://doi.org/10.12989/cac.2020.25.5.411

Ishak, A. and Nazar, R. (2009), "Laminar boundary layer flow along a stretching cylinder", *Eur. J. Sci. Res.*, **36**(1), 22-29. https://doi.org/10.5897/IJPS12.093

Ishak, A., Nazar, R. and Pop, I. (2008), "Uniform suction/ blowing effect on flow and heat transfer due to stretching cylinder", *Appl. Math. Mod.*, **32**, 2059-2066. http://doi.org/10.1016/j.apm.2007.06.036

Khadimallah, M.A., Hussain, M. and Harbaoui, I. (2020b), "Application of Kelvin's theory for structural assessment of FG rotating cylindrical shell: Vibration control", *Adv. Concr. Constr.*, **10**(6), 499-507. https://doi.org/10.12989/acc.2020.10.6.499

Khadimallah, M.A., Hussain, M., Khedher, K.M., Naeem, M.N. and Tounsi, A. (2020a), "Backward and forward rotating of FG

ring support cylindrical shells", *Steel Compos. Struct.*, **37**(2), 137-150. https://doi.org/10.12989/scs.2020.37.2.137

Khan, W.A. and Pop, I. (2010), "Boundary-layer flow of a nanofluid past a stretching sheet", *Int. Heat Mass Transf.*, **53**(11-12), 2477-2483. https://doi.org/10.1016/j.ijheatmasstransfer.2010.01.032

Konch, J. and Hazarika, G.C. (2017), "Unsteady Hydro magnetic flow of dusty fluid over a stretching cylinder with variable viscosity and thermal conductivity", *Int. J. Adv. Sci. and Tech.*, **99**, 57-70. http://doi.org/10.14257/ijast.2017.99.05.

Mahdy, A. (2015), "Heat transfer and flow of a Casson fluid due to a stretching cylinder with the soret and dufour effects", *J. Eng. Phys. Thermophys.*, **88**(4), 928-936. https://doi.org/10.1007/s10891-015-1267-6.

Malik, M.Y., Naseer, M., Nadeem, S. and Rehman, A. (2013), "The boundary layer flow of Casson nanofluid over an exponentially stretching cylinder", *Appl Nanosci*, **4**, 869-873. https://doi.org/10.1007/s 13204-013-0267-0

Naseer, M., Malik, M.Y., Nadeem, S. and Rehman, A. (2014), "The boundary layer flow of hyperbolic tangent fluid over a vertical exponentially stretching cylinder", *Alexandria Eng. J.*, **53**, 747-750. https://doi.org/10.1016/j.aej.2014.05.001

Qazaq, A., Hussain, M., Mujalli, M. and Tounsi, A. (2022), "Fundamental computer assessment of ring support with exponent of trigonometric function: Safety geometrical perfection", *Adv. Concr. Constr.*, **14**(6), 381. https://doi.org/10.12989/acc.2022.14.6.381

Rasekh, A., Ganji, D.D., Tavakoli, S., Ehsani, H. and Naeejee, S. (2014), "MHD flow and heat transfer of dusty fluid over a stretching hollow cylinder with a convective boundary conditions", *Heat Trans. Asian Res.*, **43**(3), 221-232. https://doi.org/10.1002/htj.21073

Rebhi, A.D. (2010), "On boundary layer flow of dusty gas from a horizontal circular cylinder", *Braz. J. Chem. Eng.*, **27**(4), 653-662. http://doi.org/10.1590/S0104-66322010000400017.

Rehman, A. (2015) "Boundary layer flow and heat transfer of Micropolar Fluid over a vertical exponentially stretching cylinder", *Appl. Comp. Math*, **4**(6), 424-430. http://doi.org/10.11648/j.acm.20150406.15

Safaei, B., Khoda, F.H. and Fattahi, A.M. (2019), "Non-classical plate model for single-layered graphene sheet for axial buckling", *Adv Nano Res*, **7**(4), 265-275. 10.12989/anr.2019.7.4.265

Saffman, P.G. (1962), "On the stability of laminar flow of a dusty gas", *J. Fluid Mech.*, **13**, 120-128. https://doi.org/10.1017/S0022112062000555

Salah, F., Boucham, B., Bourada, F., Benzair, A., Bousahla, A.A. and Tounsi, A. (2019), "Investigation of thermal buckling properties of ceramic-metal FGM sandwich plates using 2D integral plate model", *Steel Compos. Struct.*, **33**(6), 805-822. https://doi.org/10.12989/scs.2019.33.6.805

Salahuddin, T., Malik, M.Y., Hussain, A., Awais, M. and Bilal, S. (2017), "Mixed convection boundary layer flow of Williamson fluid with slip conditions over a stretching cylinder by using Keller-box method", *Int. J. Nonlinear Sci. Numer. Simul.*, **18**(1), 9-17. https://doi.org/10.1515/ijnsns.2015.0090

Selmi, A. and Hassis, H. (2021), "Vibration analysis of post-buckled fluid-conveying functionally graded pipe", *Compos. Part C*, **4**, 100117. https://doi.org/10.1016/j.jcomc.2021.100117

Shadravan, S., Ramseyer, C.C. and Floyd, R.W. (2019), "Comparison of structural foam sheathing and oriented strand board panels of shear walls under lateral load", *Adv. Comput. Des.*, **4**(3), 251-272. https://doi.org/10.12989/acd.2019.4.3.251

Su, Y., Iyela, P.M., Zhu, J., Chao, X., Kang, S. and Long, X. (2024), "A Voronoi-based gaussian smoothing algorithm for efficiently generating RVEs of multi-phase composites with graded aggregates and random pores", *Mater. Des.*, **244**, 113159. https://doi.org/10.1016/j.matdes.2024.113159

Sun, L., Wang, G. and Zhang, C. (2024), "Experimental investigation of a novel high performance multi-walled carbon nano-polyvinylpyrrolidone/silicon-based shear thickening fluid damper", *J. Intell. Mater. Syst. Struct.*, **35**(6), 661-672. http://doi.org/10.1177/1045389X231222999

Wang, C.Y. (1988), "Fluid flow due to a stretching cylinder", *Phys. Fl*, **31**, 466-468. https://doi.org/10.1063/1.866827

Wang, C.Y. and Ng, C.O. (2011), "Slip flow due to a stretching cylinder", *Int. J. Non Lin. Mech.*, **46**, 1191-1194. https://doi.org/10.1016/j.ijnonlinmec.2011.05

Yao, Y., Zhou, L., Huang, H., Chen, Z. and Ye, Y. (2023), "Cyclic performance of novel composite beam-to-column connections with reduced beam section fuse elements", *Structures*, **50**, 842-858. https://doi.org/10.1016/j.istruc.2023.02.054

Zhang, W., Kang, S., Liu, X., Lin, B. and Huang, Y. (2023), "Experimental and simulative analysis of flexural performance in UHPC-RC hybrid beams", *Constr. Build. Mater.*, **436**, 136889. https://doi.org/10.1016/j.conbuildmat.2024.136889

Zhu, C., Al-Dossari, M., Rezapour, S., Shateyi, S. and Gunay, B. (2024), "Analytical optical solutions to the nonlinear Zakharov system via logarithmic transformation", *Results Phys.*, **56**, 107298. https://doi.org/10.1016/j.rinp.2023.107298

CC